

# Physio-climatic controls on vulnerability of watersheds to climate and land use change across the United States

Ankit Deshmukh

A Thesis Submitted to  
Indian Institute of Technology Hyderabad  
In Partial Fulfillment of the Requirements for  
The Degree of Master of Technology



भारतीय प्रौद्योगिकी संस्थान हैदराबाद  
Indian Institute of Technology Hyderabad

Department of Civil Engineering

June 2016

## Declaration

I declare that this written submission represents my ideas in my own words, and where ideas or words of others have been included, I have adequately cited and referenced the original sources. I also declare that I have adhered to all principles of academic honesty and integrity and have not misrepresented or fabricated or falsified any idea/data/fact/source in my submission. I understand that any violation of the above will be a cause for disciplinary action by the Institute and can also evoke penal action from the sources that have thus not been properly cited, or from whom proper permission has not been taken when needed.



(Signature)

Ankit Deshmukh

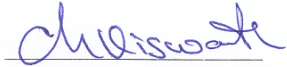
(Ankit Deshmukh)

CE14MTECH11025

(Roll No.)

## Approval Sheet

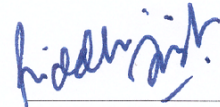
This Thesis entitled Physio-climatic controls on vulnerability of watersheds to climate and land use change across the United States by Ankit Deshmukh is approved for the degree of Master of Technology from IIT Hyderabad



(Dr. Chinthapenta R Viswanath) Examiner  
Assistant Professor  
Department of Mechanical and Aerospace Engineering  
Indian Institute of Technology Hyderabad



(Dr. Basudev Biswal) Examiner  
Assistant Professor  
Department of Civil Engineering  
Indian Institute of Technology Hyderabad



(Dr. Riddhi Singh) Adviser  
Assistant Professor  
Department of Civil Engineering  
Indian Institute of Technology Hyderabad

## Acknowledgements

First and foremost I offer my sincerest gratitude to my supervisor, Dr Riddhi Singh, who has supported me throughout my thesis. I attribute the level of my Masters degree to her encouragement and effort and without her support this thesis, would not have been completed or written. The Department of Civil Engineering has provided the support which I needed to produce and complete my thesis. I am thankful to my friends and teachers who has provided good arguments about my field and helped me achieve finest knowledge of my filed and related knowledge.

Finally, I wish to thank my parents for their love and support, without whom I would never have enjoyed so many opportunities.



# Abstract

Understanding a watersheds vulnerability to environmental (climatic and land use) change is crucial for managing such complex systems and is essential for water resources management. However, obtaining projections of streamflow under changing conditions across a variety of watersheds is challenging as every step of hydrological modeling imparts uncertainty. These ubiquitous uncertainties in projections of streamflow make it very challenging to provide useful information to water policy makers and decision makers. In this study, we attempt to identify dominant controls on watersheds vulnerability to climate and land use change independent of future projections of climate change. We propose a definition of vulnerability that can be used by a diverse range of water system managers and is useful in the presence of large uncertainties in drivers of environmental change like extreme flow conditions, as well as others that are relevant from the point of view of instream organisms.

We achieve these goals by using an exploratory modelling framework that provides approximate estimation of watershed vulnerability to change and allows user to define their own definition of vulnerability. The framework uses a parsimonious lumped model that simulates runoff at daily time steps to obtain the response of a watershed under a range of climatic and land use scenarios. The simulated runoff is used to compute four indicators - mean annual rainfall, indicators characterizing flood and droughts, and an indicator representing health of instream organisms. These indicators are classified in to different classes. Each class reflects a level of vulnerability based on stakeholders defined thresholds of acceptable change. We then use classification and regression trees (CART) to identify the ranges of climate and land use change that lead to different classes of the indicator.

In this way, we identify critical thresholds of climate and land use change that result in a vulnerable range of a streamflow indicator across 77 watersheds of the conterminous United States. Then, we use these thresholds to create a vulnerability map of US that represents spatial distribution of vulnerability across United States. This vulnerability map provides an understanding of physio-climatic settings of watersheds that are more or less vulnerable to precipitation and land use change. Such vulnerability maps can help water resource administration in the planning for watersheds that will become vulnerable even under slight changes in precipitation or land use and thus require more precise monitoring. We also employ Circos diagrams to visualize dominant controls on watersheds vulnerability, i.e., whether climate change, land use change, or hydrologic model parameters are more important in determining the vulnerability of a watershed. We find that precipitation is a key dominant control

for all the indicators considered in this analysis. We also find the flood indicator is complicated in a way that is depends of many controls, snow related parameters in the hydrologic model being one of them. In this way, we identify several interesting links between a watersheds vulnerability to environmental change and its climate, land use, and representative hydrologic model components.

# Contents

Declaration . . . . .	ii
Approval Sheet . . . . .	iii
Acknowledgements . . . . .	iv
Abstract . . . . .	v
<b>1 Introduction</b>	<b>1</b>
1.1 Towards vulnerability based approaches for managing the impacts of environmental change on water resources . . . . .	1
1.2 Generating threshold projection as vulnerability maps for the United States . . . . .	2
<b>2 Methodology</b>	<b>4</b>
2.1 Modelling framework . . . . .	4
2.2 Hydrologic model . . . . .	6
2.3 Indicators of vulnerability . . . . .	8
2.4 Threshold identification via classification and regression trees (CART)	9
<b>3 Study area and data</b>	<b>11</b>
<b>4 Results</b>	<b>13</b>
4.1 The exploratory modelling framework . . . . .	13
4.1.1 Sampling of climate and land use scenarios . . . . .	13
4.1.2 Identification of parameter ranges and behavioural parameter sets . . . . .	14
4.1.3 Identification of critical thresholds . . . . .	16
4.1.4 Threshold mapping . . . . .	18
<b>5 Discussion &amp; Conclusions</b>	<b>24</b>
<b>References</b>	<b>29</b>

# List of Figures

2.1	Modelling framework implemented to estimate vulnerability and its dependence on watershed's physio-climatic properties. (a) First, a large range of climate and land use change combinations are generated using an exploratory modelling framework. Next, each combination is used to simulate runoff using a hydrological model that accounts for parametric uncertainty. Indicators are calculated based on the simulated flow and classified into different vulnerability classes. At the end, we use CART to estimate critical climate and land use change combinations. (b) We apply exploratory modelling to a large number of watersheds and quantify critical climate and land use change thresholds for each. . . . .	5
2.2	A parsimonious hydrologic model structure used in the study which simulates runoff on daily time steps. Land use is incorporated as percentage of deep rooted vegetation in the watershed. . . . .	7
3.1	Location of the watersheds used in the study. Each circle on the map represents the centroid of the watershed. Dark colored watersheds are removed from the analysis due to low ( $<0.1$ ) runoff ratios. . . . .	12
4.1	Incorporating parametric uncertainty in the exploratory modelling framework. First, a wide range of possible values is fixed for each parameter based on literature review. Next, <i>a priori</i> parameter ranges are estimated using watershed's physical characteristics for selected parameters. Finally, the behavioural range of parameters is arrived at using NSE and percentage Bias criteria. . . . .	14

4.2	Computation of critical threshold of change for precipitation and land use using CART. The thresholds are calculated based on weighted averaged of the threshold values on leaf (end) nodes that lead to vulnerability classes. Shown is a typical output of CART for a watershed–indicator (mean annual runoff) combination. Red color denotes the class of highest vulnerability in the indicator (C3) and red dashed line represents the paths leading to C3 for this watershed. . . . .	17
4.3	Critical thresholds for precipitation reduction that leads to the highest class of vulnerability (C3) for water availability, represented by long term mean annual runoff, for each watershed. The size of the circles corresponds to the precipitation reduction that causes a transition to the vulnerable regime, colors denote aridity index. Thresholds are expressed as the ratio of critical precipitation values to historical precipitation values, both are long term means. Higher size indicates higher vulnerability as ratios closer to one or very small reductions in long term precipitation can cause a transition to C3, and vice-versa. .	19
4.4	Same as Figure 6, but for land use change. Note that not all watersheds showed land use as a significant control for water availability. Thus, the number of circles are fewer as compared to Figure 4.3 . . . . .	20
4.5	Circos plots to visualize dominant controls for each indicator–watershed combination. Controls are classified as – long term precipitation, land use parameter, long term temperature, soil parameters, and routing parameters. Each circos plot represents one indicator. The plot is created by using the information of the hierarchy order of controls from CART output of each watershed. Outer edges of the plot show each control category and all watersheds represented by their serial numbers. The purple, blue, green, and red lines that connect watershed controls and serial number, indicate a decreasing level of importance. For example, for mean annual runoff, most important control is precipitation as it has the maximum number of purple lines connected to the watersheds. . . . .	23

# List of Tables

2.1	Indicator definition and classification . . . . .	8
4.1	Feasible range for the hydrologic model parameters . . . . .	15
A	Information of watersheds used in the study. . . . .	27
B	Ranges of parameters obtained from <i>apriori</i> parameter estimation for all watersheds. . . . .	28



# Chapter 1

## Introduction

### 1.1 Towards vulnerability based approaches for managing the impacts of environmental change on water resources

Quantifying the hydrologic response of a watershed to changing climate and land use is essential for managing the water dependent ecological and economic systems in a region. There are now a plethora of studies that attempt to obtain the projections of water resources under changing climate at various spatial and temporal scales [1, 2, 3, 4, 5, 6, 7, 8]. Many efforts in this direction have culminated in the understanding that future water resources projections are ultimately dependent upon the projections of the drivers of change (land use and climate change), the type of hydrologic model used, parameter identification strategies adopted, and several such subjective decisions that are made while using the hydro-climatic chain [9, 10, 11, 12, 13, 14, 15, 16].

Typically, the resultant uncertainties in streamflow projections tend to be larger than the required precision of these projections for planning purposes [17, 18]. The presence of such large uncertainties warrants a shift in focus of problems formulated for climate change adaptation from obtaining projections to understanding what makes a watershed vulnerable to environmental change. In other words, understanding the expected sensitivity of a watershed to applied change is likely to be more beneficial than obtaining wide estimates of possible future projections of change. Past efforts at understanding watershed's sensitivity to environmental change have focused on using historically available streamflow and climate data to quantify the sensitivity [19] or have applied experimental modelling approaches [20, 21]. In either approaches, the sensitivity (or climate elasticity) is defined as the change in

watershed's response variable (streamflow) per unit change in climate.

For a complete understanding of watershed's potential response to change, the link between its sensitivity and physio-climatic setting needs to be explored. Recent efforts include the work by [22], who attempt to relate watershed's storage (approximated through its streamflow recession dynamics) with its sensitivity. There are two ways in which such relationships can be further generalized. First, sensitivity can be related to watershed's physio-climatic characteristics as opposed to a streamflow-based index, thus enabling estimations of sensitivity for ungauged catchments. Second, a decision maker is most likely interested in watershed's vulnerability to transition into a pre-defined streamflow regime, and not just its sensitivity to a unit change in climate or land use. This requires defining vulnerability in a way that allows the decision maker to guide the modelling process based on their perception of ranges of a hydrologic indicator that are acceptable [23].

Here, we propose a modelling driven approach to quantify vulnerability that allows decision makers to define a vulnerability metric based on their preferences. We build upon recently developed bottomup or exploratory modelling approaches to achieve this goal [24, 25, 26, 27, 28, 29, 30, 31, 32, 33]. Exploratory modelling assesses the response of a watershed to a large range of artificially applied changes in climate and land use. Then, the relative change in hydrologic indicators of interest as compared to their historical values are estimated across all climate and land use change scenarios. The simulated change in these indicators can then be classified as vulnerable or otherwise. A multi-tier classification is also possible [18]. Finally, by using appropriate search algorithms, the thresholds of change in climate and land use that lead to vulnerability can be estimated. Thus, the maximum tolerable climate or land use change beyond which the value of a hydrologic indicator is classified as vulnerable, can be used as a proxy for watershed's vulnerability to change.

## **1.2 Generating threshold projection as vulnerability maps for the United States**

In this study, we aim to perform an exploratory modelling analysis across a large number of watersheds across the conterminous United States to understand the vulnerability of watersheds to change. We select watersheds with a significant hydro-climatic gradient in order to perform the comparative analysis. We simulate the dynamic response of a watershed across a large number of climate and land use change com-

binations. Using these simulations, we quantify various hydrologic indicators that determine water availability in the region, occurrence of flood and droughts, and also the survivability of instream organisms. We then determine the critical thresholds of climate and land use change for each indicator. These critical thresholds are a proxy for vulnerability of watersheds to change. The spatial variability of these vulnerabilities is then analyzed to identify the spatial distribution of vulnerable watersheds. We also analyze the multidimensional dataset obtained from the exploratory modelling exercise across 77 using Circos plots for interpreting complex controls on watershed vulnerability to change.

# Chapter 2

## Methodology

### 2.1 Modelling framework

We adopt the exploratory modelling framework proposed by [18] with modifications in sampling strategies of the climate and land use space and parameter uncertainty quantification (Figure 2.1a).

We begin by defining feasible ranges of climate and land use change, which is shown by the cube in the left side of Figure 2.1a. The climate scenarios are a combination of precipitation and temperature change scenarios while land use change is represented as a parameter in the hydrologic model used in the analysis. To generate the climate scenarios, we use the delta change method in which mean of climate variables (precipitation and temperature) are changed keeping higher order moments fixed. Scenarios of land use change are implemented by changing a parameter representing the fraction of deep rooted vegetation cover in the hydrologic model between 0 and 1. These climates and land use change scenarios are then propagated through a hydrologic model that incorporates parametric uncertainties. We discuss the method for incorporating the uncertainties associated with parameter sets in Section 4.1.1. Thus, the total number of streamflow simulations explored for each watershed can be estimated as:

$$N = P \times T \times L \times \Theta$$

where,  $P$  is the number of precipitation change scenarios,  $T$  is the number of temperature change scenarios,  $L$  is the number of land use change scenarios, and  $\Theta$  is the number of parameter sets considered.

Next, we estimate a hydrologic indicator of interest for each streamflow simulation. Once the indicators are estimated, their values are classified into different categories based on pre-specified thresholds. Here, we employ indicators that rep-

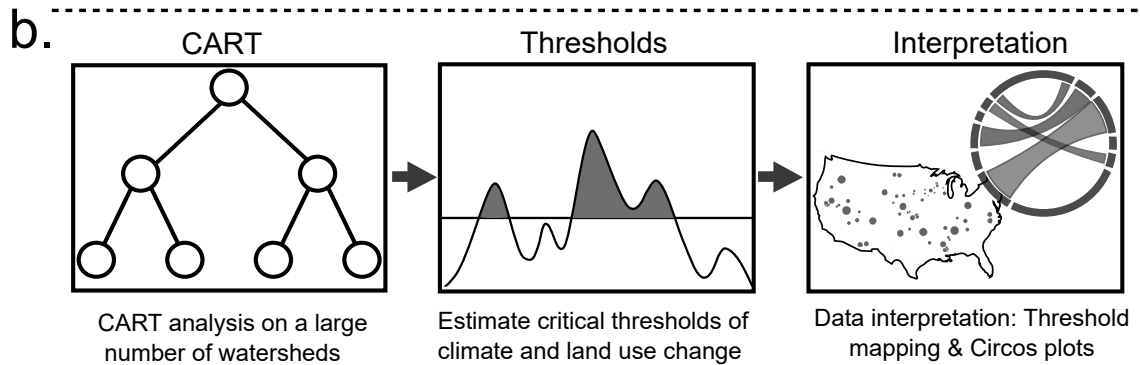
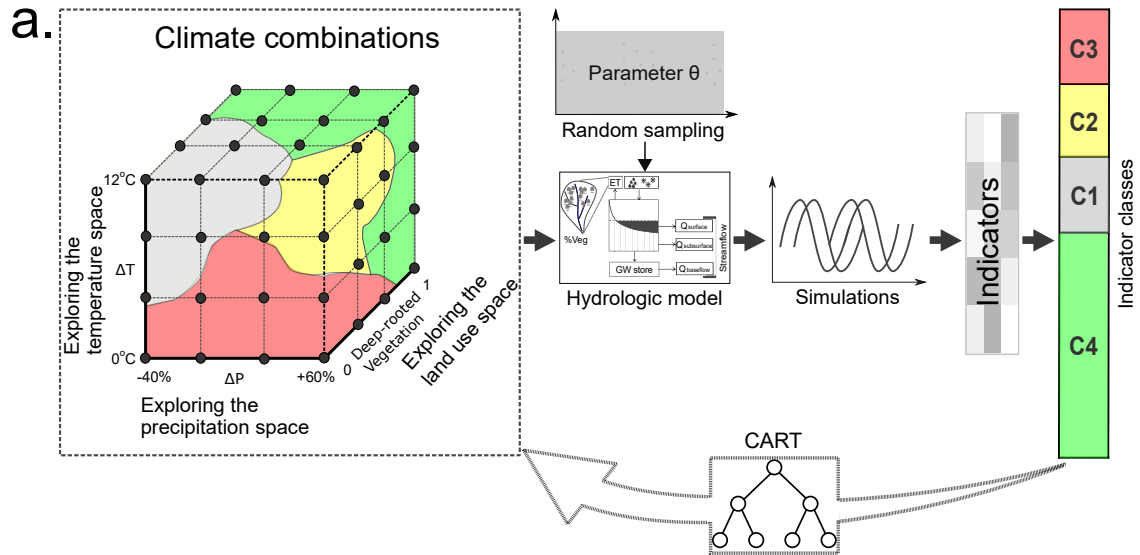


Figure 2.1: Modelling framework implemented to estimate vulnerability and its dependence on watershed’s physio-climatic properties. (a) First, a large range of climate and land use change combinations are generated using an exploratory modelling framework. Next, each combination is used to simulate runoff using a hydrological model that accounts for parametric uncertainty. Indicators are calculated based on the simulated flow and classified into different vulnerability classes. At the end, we use CART to estimate critical climate and land use change combinations. (b) We apply exploratory modelling to a large number of watersheds and quantify critical climate and land use change thresholds for each.

resent water availability, hydrologic extremes, and ecologically relevant indices. We chose these categories based on literature review, wherever information regarding the critical ranges of the indicators was available. In absence of literature specified critical thresholds, we estimated the percentage change in estimated indicator w.r.t its historical values that are obtained by using observed stream flow data. These changes are then categorized based on an assumed classification scheme. Note that in a real application, these classes will be provided by the decision maker. Following this, classification and regression trees (CART) identify the regions in the input space that lead to vulnerable classes. This provides a way to estimate the critical values of climate and land use changes that lead to vulnerability. For example, in Figure 2.1, an indicator is classifying into four classes (each class represented with a color) and using CART, the climate and land use combinations that lead to vulnerability can be determined.

## 2.2 Hydrologic model

We use a spatially lumped form of a parsimonious rainfall runoff model that simulates streamflow at daily time steps (Figure.2.2).

The model has a basic representation of land use in the form of percent of deep rooted vegetation that can be altered to simulate land use change. The model structure is adopted from parsimonious structures suggested by [34], and used further by [35]. The model comprises of a snow module, a soil moisture accounting module, and a routing module. The snow module is based on the degree-day method that uses three parameters to estimate snow storage and melt. The snow module takes in daily precipitation and provides fluxes of daily melt and rainfall, which are then passed on to the soil moisture accounting (SMA) module. The SMA module comprises of multiple buckets in parallel configuration, and employs the saturation excess mechanism of fill and spill to generate effective rainfall [36, 35]. Evapotranspiration is also estimated in the SMA based on the parameters that determine the leaf area index and percentage of deep rooted vegetation cover, with impact of phenology adopted from [37]. The land use change parameter divides the watershed area into bare soil and deep rooted forest cover, and evapotranspiration over each is estimated separately [34]. For more details, readers are referred to [18].



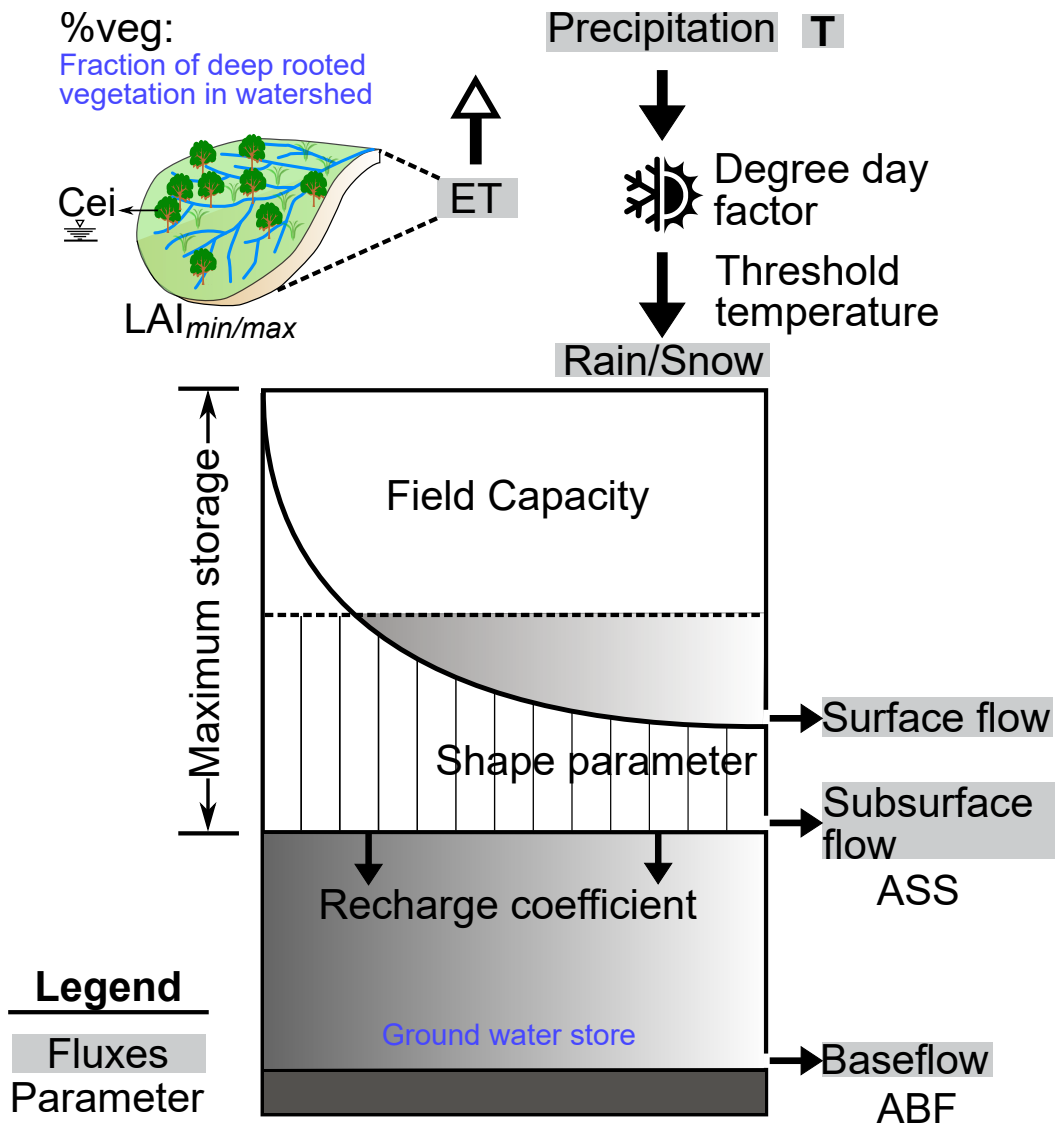


Figure 2.2: A parsimonious hydrologic model structure used in the study which simulates runoff on daily time steps. Land use is incorporated as percentage of deep rooted vegetation in the watershed.

## 2.3 Indicators of vulnerability

We use three hydrologic indicators that represents average, low flow, and high flow conditions in the watershed [Table 2.1].

Table 2.1: Indicator definition and classification

No.	Indicator	Description	Class definition
1	Mean annual runoff	Mean annual flow (normalized by catchment area) , MA41 [38]: This indicator represents general water availability.	Reduction in streamflow C1: 0% to -25% C2: -25% to -50% C3: <-50% C4: >0%
2	Flood	Mean number of high flow events per year (an upper threshold of 3 times median flow over all years), FH6 [38] : It represents frequency of high flow	Flood flow C1: 0% to 25% C2: 25% to 50% C3: >50% C4: <0%
3	FPIFR	Proportion of index flow (Median August discharge divided by mean annual discharge) removed. [38]	Index flow removed C1: <0.2 C2: 0.2 to 0.4 C3: >0.4
4	Drought	Streamflow Drought Index (SDI) [39].	Based on ranges of SDI C0: $SDI \geq 0.0$ C1: $-1.0 \leq SDI < 0.0$ C1: $-1.5 \leq SDI < 1.0$ C1: $-2.0 \leq SDI < 1.5$ C4: $< -2.0$

These are mean annual flow, frequency of flooding, and duration of low flow, respectively. Definition frequency of flooding is adopted from [38]. Drought indicators is defined based on stream flow drought index (SDI) [39]. Based on SDI, hydrologic drought classified in 5 categories 0 to 4. This index needs only streamflow for its estimation as it is based on the cumulative volume of stream flow for overlapping period of three, six, nine, and twelve months within a hydrologic year [39]. In addition, a hydrologic indicator that relates fish population to streamflow (FPIFR) is also used. The indicator is proportion of index flow removed, where index flow is specified as median August discharge divided by the mean annual discharge [40, 41].

A watershed’s vulnerability to environmental change is defined on the basis of relative change in indicator magnitude in a change scenario as compared to the his-

torically observed indicator value. For example, based on the assumption that mean annual flow is a proxy for water availability in the watershed, it is assumed to become vulnerable if its values fall below historically observed values. Once the values decrease beyond a threshold, the vulnerability class is changed. In this way, four vulnerability classes are defined for mean annual runoff. Reductions in mean annual runoff as compared to historical value is classified as C1, C2, or C3, with each class spanning a range of successive 25% reductions. Increases in mean annual runoff is classified as C4. Similarly, we classify frequency of flooding into four classes. Successive relative increases are assigned to classes C1, C2, and C3 while decreases are assigned to C4 (Table 2.1). For FPIFR and the drought indicator, we use pre-defined class definitions from past literature. Class definitions of the drought indicator were acquired from [39]. Drought indicator is classified into five classes C0–C4 based on the values of streamflow drought index(SDI). C0 represents no drought and C4 indicates extreme drought. Class definition for FPIFR are adopted from [41], who classify FPIFR into three classes – C1, C2, and C3. C1 is proportion of index flow removed which can cause reduction in 10% initial fish population.

## 2.4 Threshold identification via classification and regression trees (CART)

Each indicator class is a result of possible combinations of climate change, land use change, and parameter sets. Classification and regression trees (CART) allow us to identify the space of climate, land use and hydrologic model parameters that lead to vulnerable classes of indicators. CART is a binary recursive partitioning algorithm that divides multiple variable input space into subspaces and each subspace is related to an output indicator class [42]. To implement CART, we use the statistical classification and regression tree package in R, "rpart" [43]. 'rpart' also performs a tenfold cross validation of the CART trees to ensure that the final structure of the trees is not over-fitted to the data. The output of CART provides a series of logical yes/no type decisions such that the input space that results in a certain class of indicators is identified. We use CART to relate categories for all four indicators to the input space of climate, land use, and parameter sets. This enables us to identify the ranges of input variables that lead to a high vulnerability of the indicator of interest. Thus, critical thresholds are estimated as the values of climate (precipitation and temperature) or land use change that lead to a vulnerable class for a given hydrologic

indicator.

# Chapter 3

## Study area and data

We implement the CART analysis to identify critical thresholds for climate and land use change across 77 watersheds in the conterminous United States (Figure 3.1).

The hydro meteorological data sets used in this study were developed as part of the Model Parameter Estimation Experiment (MOPEX) [44]. These watersheds represent the largest set of watersheds from the MOPEX database with an overlapping period of 10 years for the streamflow data from 1959-1968 [45]. All watersheds are reference watersheds, i.e., they are classified as minimally impacted in the Falcone database [46]. Three primary criteria are used to identify reference watersheds: a quantitative index of anthropogenic modification within the watershed based on GIS derived variables, visual inspection of every stream gage and drainage basin from recent high resolution imagery and topographic maps, and information about man-made influences from USGS Annual Water Data Reports. We found seven watersheds in this database with historical runoff ratio less than 0.1, and removed them from further analysis as the hydrologic model employed in this analysis is not likely to represent the hydrologic processes in these semi-arid watersheds adequately. A summary of watershed related information is provided in appendix Table-A. Watershed characteristics for *a priori* parameter identification are obtained from the Falcone database [46].

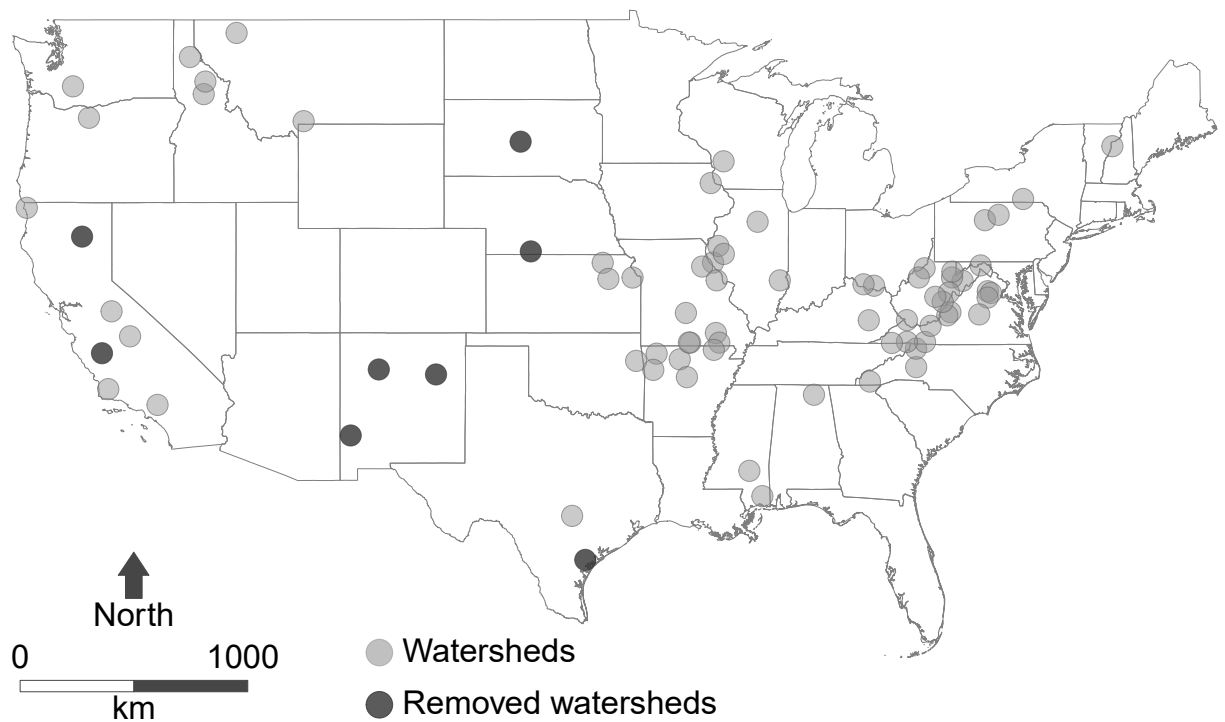


Figure 3.1: Location of the watersheds used in the study. Each circle on the map represents the centroid of the watershed. Dark colored watersheds are removed from the analysis due to low ( $<0.1$ ) runoff ratios.



# Chapter 4

## Results

We begin the result section by presenting the implementation details of the exploratory modelling framework (Section 4.1) such as the sampling of climate and land use scenarios (Section 4.1.1), parameter uncertainty estimation method (Section 4.1.2), and method for estimation of critical thresholds (Section 4.1.3). This is followed by the first main result - the spatial mapping of vulnerability of watersheds to climate and land use change for mean annual flow for the conterminous US (Section 4.1.4).

### 4.1 The exploratory modelling framework

#### 4.1.1 Sampling of climate and land use scenarios

We generate a large number of climate combinations using delta change method which is describe in section 2.1. Precipitation scenarios are generated by varying the precipitation time series within -40% to +60% of its historical value, and temperature change scenarios are generated by adding 0 °C to 12 °C of temperature increases to the historical time series. The precipitation and temperature change values are selected such that they are wide enough to incorporate the maximum change over a long time period as reported in the fifth assessment report of the International Panel for Climate Change [47]. We vary the parameter representing land use between 0 to 1 (completely bare soils to full vegetation cover). Precipitation, temperature, and land use changes are applied in increments of 10%, 1 °C, and 0.1, respectively. This results in 1859 combinations of potential climate and land use changes ( $13 \times 13 \times 11$ ). Each scenario is further combined with uncertain hydrologic model parameters as described next.

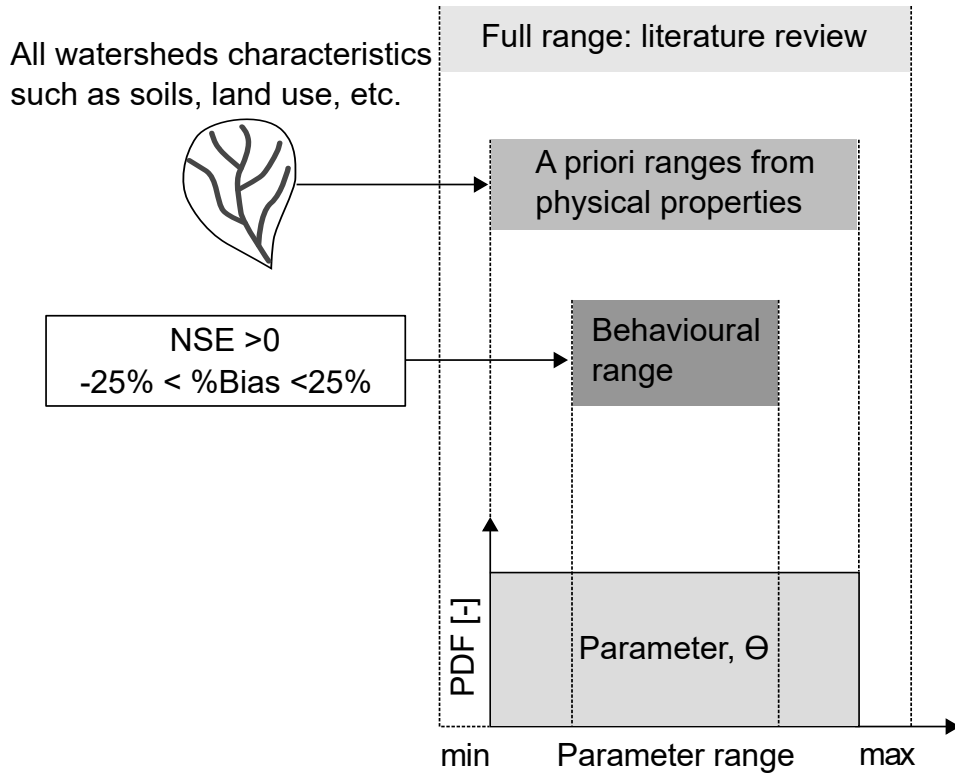


Figure 4.1: Incorporating parametric uncertainty in the exploratory modelling framework. First, a wide range of possible values is fixed for each parameter based on literature review. Next, *a priori* parameter ranges are estimated using watershed’s physical characteristics for selected parameters. Finally, the behavioural range of parameters is arrived at using NSE and percentage Bias criteria.

#### 4.1.2 Identification of parameter ranges and behavioural parameter sets

Parametric uncertainty is incorporated in analysis using by using a three step process for uncertainty identification (Figure 4.1).

We begin with a literature survey to identify the feasible range of each parameter. The model has a total 13 parameters including one representing land use. Then, we compute *a priori* parameter ranges for six of these parameters (Sb, Fc, LAImin, LAImax, ASS, ABF) while others are fixed at their full range (Table 4.1) [34, 48, 35, 49, 18]. *A priori* parameter ranges are estimated by two different ways: by using observed physical characteristics of watersheds obtained from Falcone database (for Sb, Fc, LAImin, LAImax), and, by recession curve analysis using historical streamflow data for recession parameters (ASS, ABF) (See [18] for more details). The *a priori* range for land use is fixed at the historically observed land use values. The *a priori*

ranges for parameters of each watershed are listed in appendix Table-B

Table 4.1: Feasible range for the hydrologic model parameters

	Parameters	Description	Feasible ranges		Units
			lower	upper	
<b>Soil</b>	Sb	maximum depth of soil store.	0	2000	<i>mm</i>
	B	shape factor of distribution bucket.	0	7	[-]
	Fc	threshold storage parameter	0	1	[-]
	Kd	deep recharge coefficient from the upper saturated zone to the deep store	0	0.5	[-]
<b>Vegetation</b>	% Veg	fraction of catchment area covered by deep rooted vegetation	0	1	[-]
	LAI <sub>max</sub>	maximum Leaf Area Index	0	6	<i>mm</i>
	LAI <sub>min</sub>	minimum Leaf Area Index	0	6	<i>mm</i>
	Cei	maximum canopy interception	0	0.49	<i>mm</i>
<b>Routing</b>	ASS	recession coefficient for saturated soil	0.05	0.5	<i>day</i> <sup>-1</sup>
	ABF	recession coefficient for groundwater	0.001	0.05	<i>day</i> <sup>-1</sup>
<b>Snow</b>	Ddf	degree day factor	0	20	<i>mm</i> °C <sup>-1</sup> <i>day</i> <sup>-1</sup>
	Tth	Threshold factor for snow formation	-5	5	°C
	Tb	base temperature for snow melt	-5	5	°C

Next, we generate 50000 parameter sets using the Latin hypercube sampling method by assuming uniform distribution of parameters within *a priori* ranges. We further constrain these parameter sets by testing their ability to reproduce magnitude and variability of historically observed streamflow, quantified through Nash Sutcliffe efficiency(NSE) and volumetric bias. Parameter sets producing NSE greater than 0 and a percentage volumetric bias within 25% are accepted as behavioural. After identifying the behavioural parameter sets, we select top 50 sets based on NSE performance (or the number producing a positive NSE if less than 50 sets produce positive NSE). In this manner, we end up with a maximum of 92,950 (1859 x 50)

combinations of climate, land use, and parameter sets for each watershed. Note that for watershed USGS gauge ID:011355500, we are unable to identify any parameter set that satisfies the aforementioned conditions. Thus, we exclude this watershed from further analysis, reducing the total number of watersheds we analyses to 69.

### 4.1.3 Identification of critical thresholds

Once we identify the ranges for climate and land use change along with uncertainty estimates for hydrologic model parameters, we run the hydrologic model to simulate the streamflow and estimate the hydrologic indicators of interest. This is followed up by categorization of these indicators based on predefined class definitions. Then, CART is used to partition the input space of climate, land use, and parameters to identify regions that lead to vulnerable values of hydrologic indicator. The CART output is then used to estimate the critical values of the input variables.

A typical output from CART analysis for War Eagle Creek watershed near Hindsville, AR, USGS gauge ID 07049000, is shown in Figure 4.2.

The figure outlines the process of estimating the critical values of precipitation change that lead to vulnerable class C3 for mean annual runoff for this watershed. We term this value *the critical precipitation change threshold* for mean annual runoff to transition to C3. We begin by identifying all leaf (end) nodes that result in a vulnerable class (C3). Then, the values of precipitation change that lead to the vulnerable class are noted along with the total number of simulations that belong to each end node. The critical threshold is then calculated as the weighted average of precipitation change values resulting in the end nodes with vulnerable class, using the number of simulations of each end node as weights. For the example watershed in Figure 4.2, the critical precipitation change threshold estimate turns out to be 0.757. Note that this value is expressed as a multiplier on the historical precipitation and represents a 24.3% reduction in precipitation. We thus conclude that if precipitation falls below this threshold, the mean annual runoff is likely to transition to a vulnerable regime, which in this case represents a reduction greater than 50% of the historical value.

When expressed as a ratio, values of critical precipitation change threshold close to one indicate a more vulnerable watershed for mean annual runoff. For example, if two watersheds display a critical precipitation change threshold of 0.6, and 0.9, respectively, the second watershed is more vulnerable to climate change for mean annual runoff. This is because a smaller reduction in precipitation would be required

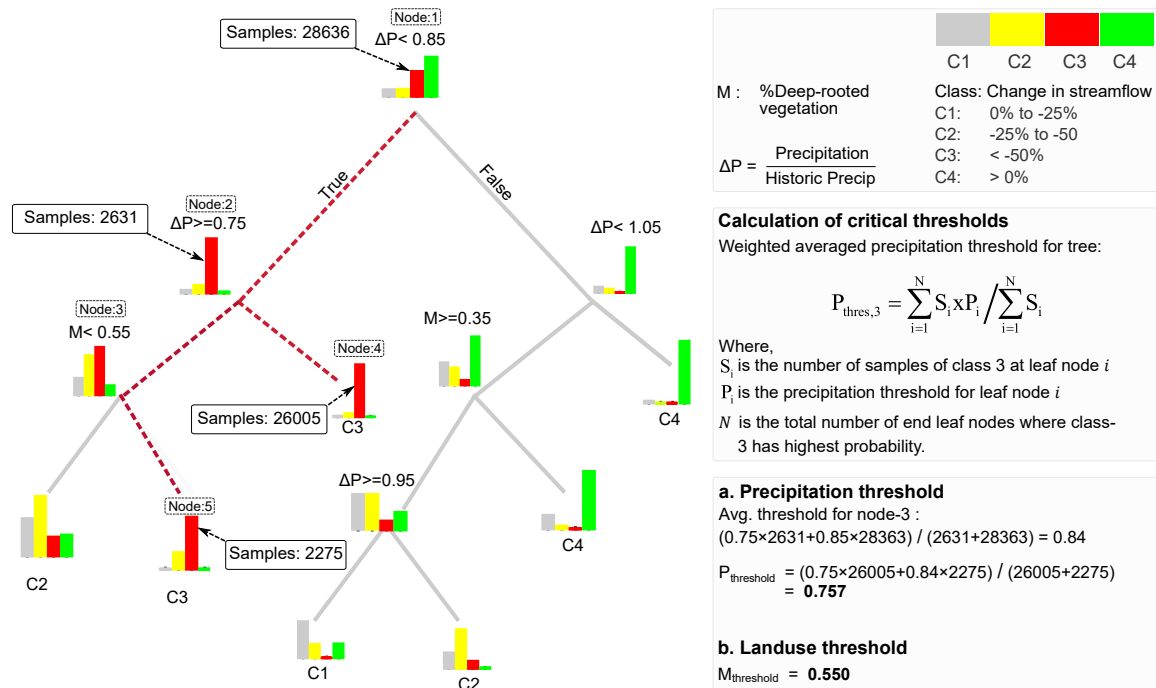


Figure 4.2: Computation of critical threshold of change for precipitation and land use using CART. The thresholds are calculated based on weighted averaged of the threshold values on leaf (end) nodes that lead to vulnerability classes. Shown is a typical output of CART for a watershed-indicator (mean annual runoff) combination. Red color denotes the class of highest vulnerability in the indicator (C3) and red dashed line represents the paths leading to C3 for this watershed.

to cause this watershed to transition to a vulnerable regime. We also found that temperature appeared in the CART output less frequently than precipitation and thus focus on precipitation change to represent climate change in the watersheds.

The critical land use change threshold is estimated as 0.55 from Figure 4.2 on similar lines. This number is the fraction of deep-rooted vegetation cover in the watershed above which mean annual runoff transitions to a vulnerable regime. Recall that the land use parameter is varied from 0 to 1 (bare soils to full coverage of deep-rooted vegetation). Thus a land use threshold of 0.55 implies that if more than 55% of the watershed is covered by deep rooted vegetation, the increased evapotranspiration is likely to reduce the mean annual runoff by more than 50% thereby cause it to transition to the vulnerable class. It is important to stress here that this land use change threshold is applicable only for the range of precipitation changes (15% to 25% reductions) that lead to the node containing land use change as the split parameter.

#### 4.1.4 Threshold mapping

We begin by discussing the spatial variability of critical precipitation change and land use thresholds for mean annual runoff that is a proxy for the overall water availability in the watersheds (Figure 4.3 & Figure 4.4). Figure 4.3 shows the critical threshold of precipitation change, where each circle represents a watershed and the magnitude of critical threshold is represented by size of circle.

Increasing size of circles indicates increasing vulnerability, as value closer to 1 are more vulnerable. We cluster critical precipitation change thresholds into 4 groups with ranges 0.55–0.70, 0.70–0.80, 0.80–0.90, and 0.90–1.05 with 21, 30, 8, and 10 watersheds falling in each group, respectively. We also find that watersheds with lower aridity index tends to be less vulnerable to precipitation change and vice versa. The spatial patterns also emphasize that watersheds in close proximity can also have significantly different critical thresholds.

On analyzing the critical threshold for land use, we find that only 40 watersheds show CART output with land use leading to vulnerable class C3. We show the spatial variation of these land use thresholds in Figure 4.4, where, the size of each circle represents vulnerability of a watershed to land use change. On categorizing the land use thresholds using the ranges 0.25–0.35, 0.35–0.45, 0.45–0.55, and 0.55–0.65, we find 4, 6, 21, and 9 watersheds fall into these classes, respectively. We also notice that watersheds with lower aridity index seem more vulnerable to land use change.

Another source of information regarding the control of watershed properties on



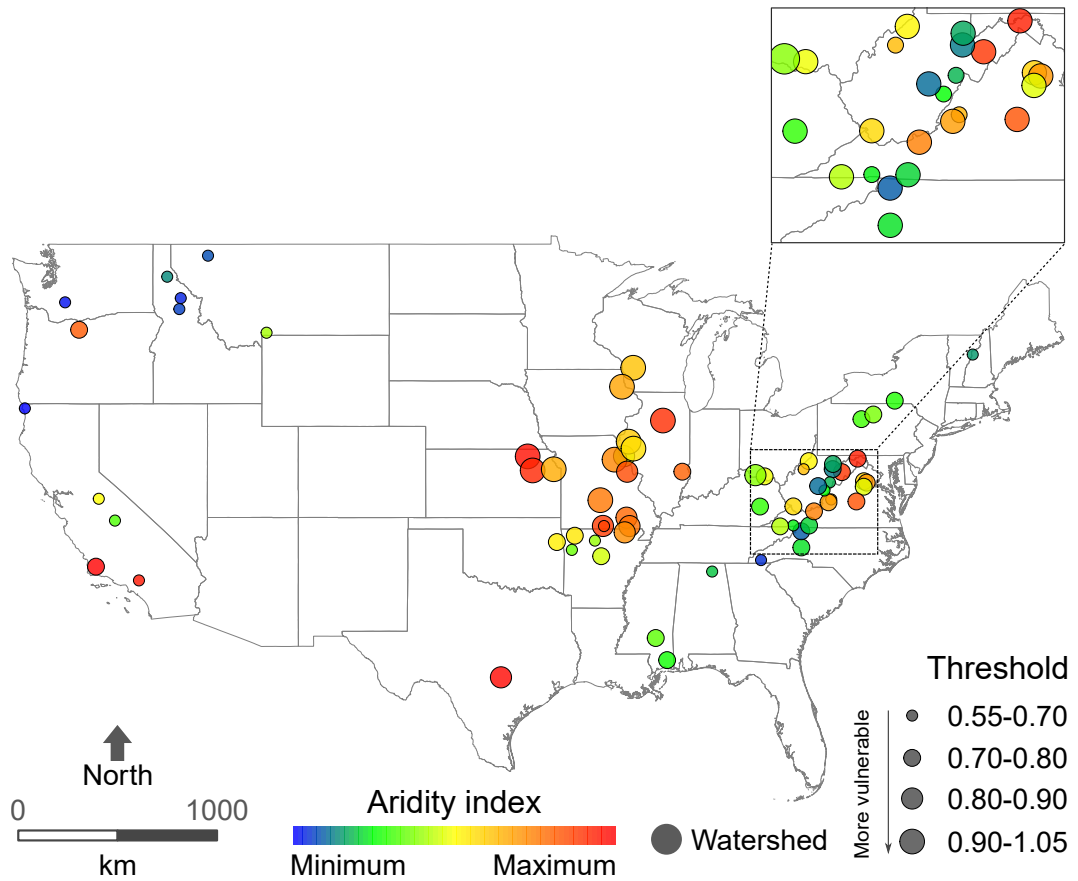


Figure 4.3: Critical thresholds for precipitation reduction that leads to the highest class of vulnerability (C3) for water availability, represented by long term mean annual runoff, for each watershed. The size of the circles corresponds to the precipitation reduction that causes a transition to the vulnerable regime, colors denote aridity index. Thresholds are expressed as the ratio of critical precipitation values to historical precipitation values, both are long term means. Higher size indicates higher vulnerability as ratios closer to one or very small reductions in long term precipitation can cause a transition to C3, and vice-versa.

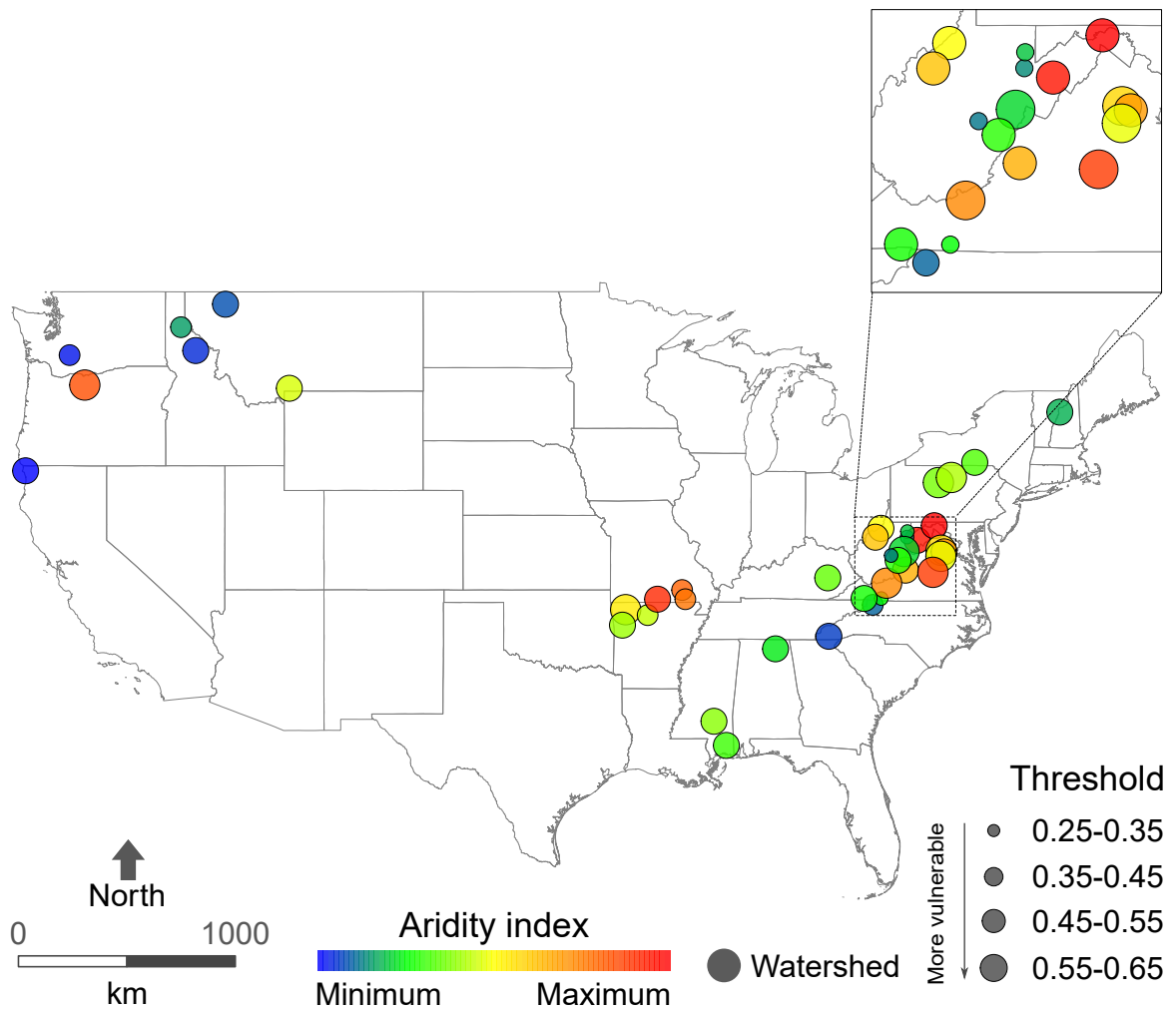


Figure 4.4: Same as Figure 6, but for land use change. Note that not all watersheds showed land use as a significant control for water availability. Thus, the number of circles are fewer as compared to Figure 4.3

critical climate or land use change threshold is provided in the CART output. Each tree presents a hierarchy of controls for each indicator-watershed combination. Visualization the outputs of the all trees would be challenging, so here we resort to Circos diagrams for circular representation of tabular data of vulnerability for better understanding and visualization (Figure 8) (see also [50]). Impact of different controls on watersheds vulnerability are shown by Circos diagrams created by the Circos tool which is developed by [51].

Circos uses a circular ideogram layout to facilitate the display of the relationships between a pair of variables represented through their position on a circle, by the use of ribbons or chords. Ranking of controls is estimated for each indicator across all watersheds based on the hierarchy of controls from the CART output. For example, if CARTs first node is precipitation, we assign precipitation as primary control for that particular indicator-watershed combination. Similarly, we determine secondary, tertiary and higher order controls. Thus, primary splits are assumed to have a higher impact on watershed vulnerability as they provide maximum information gain while splitting the space of indicator responses [42].

In this way, controls for each indicator are plotted in separate chord diagrams (Figure 8). On the outer periphery of the circles in the Circos diagram, we present controls (dark blue) and watersheds (black) considered in study. Each CART output is a result of varying the climate and land use in the watershed in the presence of parametric uncertainties. Thus, we consider six controls: precipitation change, temperature change, land use change represented by a model parameter, followed by parameters related to snow, soil, and routing, respectively. A total of 69 watersheds are shown in the chord diagram. The color of strips inside the circle represent the order of splits as obtained from the CART output. For mean annual runoff, all the watersheds have precipitation as the primary as well as secondary split indicating that it is a main control on mean water availability in a basin. A few watersheds have land use change on their secondary splits and several have it on their tertiary split, indicating that it is the second most important control on this indicator. The impact of hydrologic model parameters related to snow, soil and routing, have negligible impact on mean annual runoff. A small number of watersheds also show temperature as the tertiary control.

As opposed to mean annual runoff, the flood indicator shows a far more diverse range of controls. Precipitation is a dominating control for this indicator too, but here land use change emerges as a primary control for a significant number of watersheds. Hydrologic model parameters related to soil, and routing emerge as tertiary

controls for several watersheds. We can also find snow related parameters appearing as secondary and tertiary controls for a significant number of watersheds. We thus hypothesize that this is likely due to the role of snow melt in inducing flood response for some watersheds. Overall, we find that the controls on flood indicator are very complex. The FPIFR and drought indicators are related to low flow and show similar controls. From their Circos diagrams, we find that the primary control on these indicators is precipitation change followed by land use change. For FPIFR, hydrologic parameters related to soils and routing also have significant. FPIFR seems to be more affected by land use change than the drought indicator as indicated by the higher number of watersheds showing land use change as a secondary indicator for FPIFR.

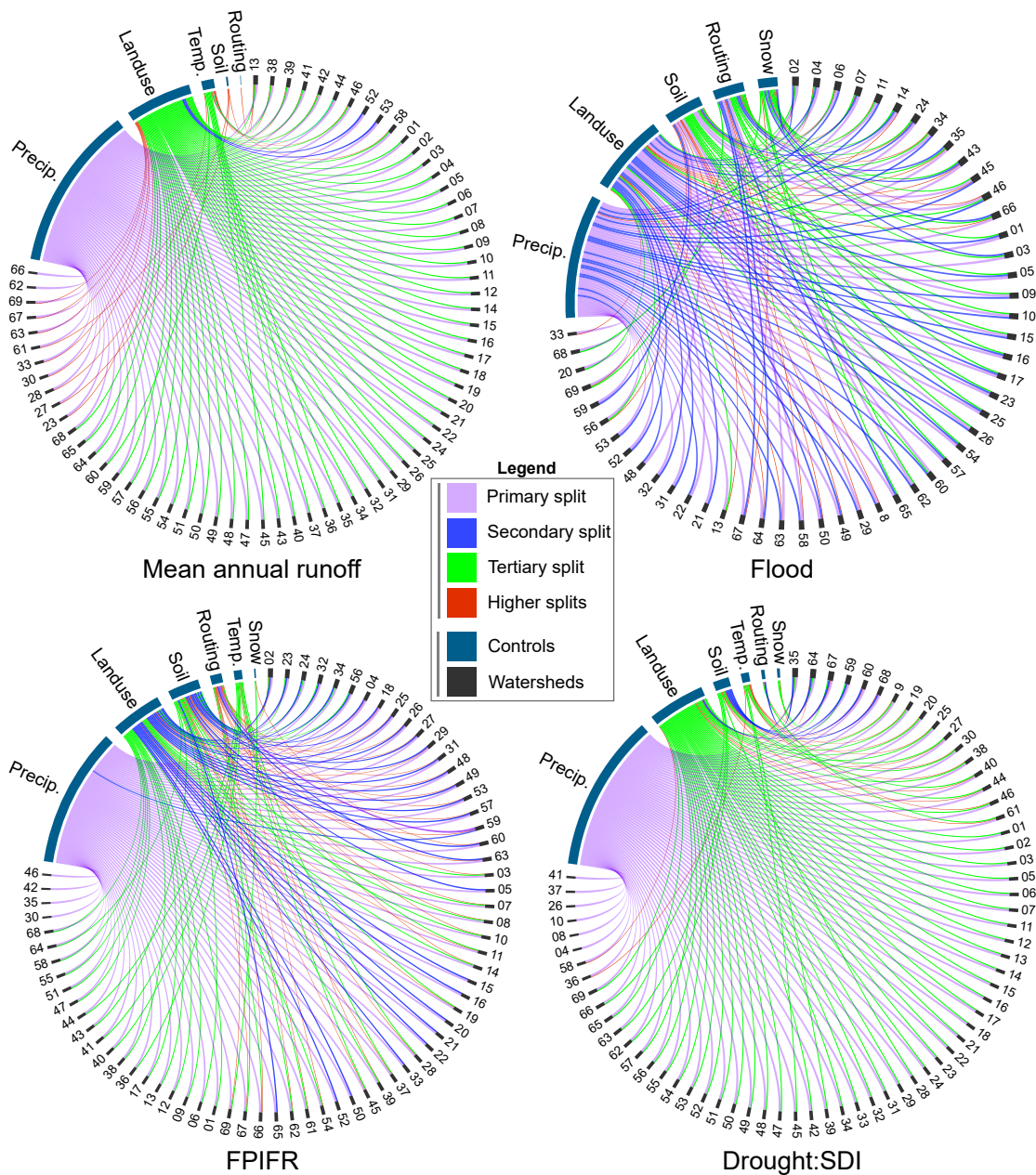


Figure 4.5: Circos plots to visualize dominant controls for each indicator–watershed combination. Controls are classified as – long term precipitation, land use parameter, long term temperature, soil parameters, and routing parameters. Each circos plot represents one indicator. The plot is created by using the information of the hierarchy order of controls from CART output of each watershed. Outer edges of the plot show each control category and all watersheds represented by their serial numbers. The purple, blue, green, and red lines that connect watershed controls and serial number, indicate a decreasing level of importance. For example, for mean annual runoff, most important control is precipitation as it has the maximum number of purple lines connected to the watersheds.

# Chapter 5

## Discussion & Conclusions

In this study, we have attempted to identify dominant controls on watersheds vulnerability to climate and land use change. The spatial variability of the identified critical thresholds across the United States gives an understanding of watersheds vulnerable to precipitation and land use change. The vulnerability map can help water resource administration in the planning of those watershed who will become vulnerable even slight change in precipitation or land use and required more precise monitoring.

We find that the vulnerabilities of watershed to environmental change varies a lot even if watersheds are situated near to each other. The vulnerability map for critical precipitation thresholds for mean annual runoff also shows that watersheds with lower aridity index are less vulnerable to precipitation change. In other words, we find that watershed with lower aridity index are less likely to transition into vulnerable regime with small change of precipitation in watershed and thus are more resilient to climate change. On the other hand, the vulnerability map for land use change thresholds does not show the same pattern. The analysis of land use change thresholds across the study watersheds shows that most watersheds will become vulnerable if percentage of deep rooted vegetation cover in a watershed exceeds 45%. Similarly, vulnerability maps for other indicators can be developed using the stakeholder based definition for critical threshold of the respective indicator.

Finally, we employ Circos diagrams for each indicator to visualize dominant controls on the indicators vulnerability to climate and land use change. Mean annual runoff, an indicator of average water availability in a watershed, shows a very distinct pattern of control: long term precipitation is a dominant control for all watersheds. This indicates that the sensitivity of water availability in streams is most dependent on precipitation change (among controls such as precipitation change, temperature change, and hydrologic model parameters). Another important control on mean an-

nual runoff that was identified using Circos plot is the long-term land use change. This control, however, ranked lower than precipitation change in most watersheds.

We show that Circos plots are especially useful to identify secondary and tertiary level controls on the watersheds vulnerability such as temperature change, soil and routing related parameters of the hydrologic model, etc. For example, we show that for mean annual runoff, temperature is only a moderate control for the watersheds. We also find that the flood indicator is one of the most complex indicator that depends on a large range of controls. Apart from precipitation and land use change, hydrologic model parameters describing soils, routing characteristics and snow formation and melt are significant drivers of watershed vulnerability to flooding.

There are a few methodological choices that can be further improved in order to strengthen the results obtained here. First of all, landuse change is simulated via a single parameter in the hydrologic model. We know that land use change has complex impacts on hydrologic properties and this rather simple representation is likely to limit the generality of our results related to vulnerability of indicators to land use change [52, 53, 54]. In addition, catchments are heterogeneous systems and using a lumped model is likely to hide the potential diverse response within a catchment to change drivers. For example, [21] pointed out that the degree of sensitivity varies with elevation even in a small catchment.

Finally, our simulated climate change scenarios merely represent a mean change in climate properties while in reality catchments around the world are undergoing change in both frequency and mean values of precipitation [IPCC], [47]. Thus, a weather generator that allows us to sample different hydrologically relevant climatic properties such as duration of dry consecutive dry/wet days, frequency of wet/dry spells, in addition to the mean values of climate variables would allow us to provide assessment of vulnerability of watersheds to changings in characteristics of the climate [55]. Nevertheless, several results from our analysis are in agreement with previous literature, which lends a degree of validity to this analysis.

Our framework can be used as a tool for comparative hydrologic analysis to identify sensitivity of watershed to various watershed physio climatic characteristics based on stockholders definition of vulnerability.

# Appendix



ID	USGS ID	Basin name	Area (km <sup>2</sup> )	Avg. elevation (m)	M.A. P (mm)	M.A. Q (mm)	M.A. PE (mm)
01	01138000	Ammonoosuc River near Bath, NH	1023	138	1018	500	824
02	01514000	Owego Creek near Owego NY	479	250	849	515	869
03	01543500	Sinnemahoning Creek at Sinnemahoning, PA	1774	235	927	459	982
04	01548500	Pine Creek at Cedar Run, PA	1564	238	869	410	939
05	01606500	South Branch Potomac River near Petersburg, WV	1686	295	876	331	1102
06	01611500	Cacapon River near Great Cacapon, WV	1748	139	831	263	1137
07	01663500	Hazel River at Rixeyville, VA	738	88	980	337	1159
08	01664000	Rappahannock River at Remington, VA	1603	77	956	311	1158
09	01667500	Rapidan River near Culpeper, VA	1212	74	1008	299	1138
10	02016000	Cowpasture River near Clifton Forge, VA	1194	307	950	349	1132
11	02018000	Craig Creek at Parr, VA	852	302	929	349	1113
12	02030500	Slate River near Arvonnia, VA	585	73	973	290	1206
13	02143000	Henry Fork near Henry River, NC	215	272	1322	546	1225
14	02472000	Leaf River Nr Collins, MS	1924	60	1349	464	1438
15	02479300	Red Creek at Vestry, MS	1142	6	1498	602	1481
16	03069500	Cheat River near Parsons, WV	1870	485	1258	789	1007
17	03070000	Cheat River at Rowlesburg, WV	2432	417	1256	800	1018
18	03114500	Middle Island Creek at Little, WV	1186	192	1002	416	1149
19	03155500	Hughes River at Cisco, WV	1173	185	989	397	1176
20	03161000	South Fork New River near Jefferson, NC	531	810	1362	706	1011
21	03164000	New River near Galax, VA	2955	673	1198	563	1060
22	03173000	Walker Creek at Bane, VA	774	508	894	336	1092
23	03180500	Greenbrier River at Durbin, WV	344	823	1132	498	965
24	03182500	Greenbrier River at Buckeye, WV	1399	636	1098	486	1047
25	03186500	Williams River at Dyer, WV	332	669	1316	859	1028
26	03213000	Tug Fork at Litwar, WV	1305	285	997	341	1176
27	03237500	Ohio Brush Creek near West Union OH	1002	156	962	370	1102
28	03238500	White Oak Creek near Georgetown OH	565	184	978	323	1076
29	03281500	South Fork Kentucky River at Booneville, KY	1870	196	1169	478	1230
30	03346000	North Fork Embarras River near Oblong, IL	824	139	921	231	1134
31	03473000	S F Holston River near Damascus, VA	785	546	1201	528	1114
32	03490000	N F Holston River near Gate City, VA	1738	365	1055	440	1174
33	03504000	Nantahala River near Rainbow Springs, NC	134	937	1961	1373	1150
34	03574500	Paint Rock River near Woodville AL	829	174	1447	776	1276
35	05408000	Kickapoo River at La Farge, WI	689	238	782	227	929
36	05412500	Turkey River at Garber, IA	4002	193	792	213	946
37	05502040	Hadley Creek at Kinderhook, IL	188	143	949	236	1067
38	05507500	Salt River near Monroe City, MO	5776	159	916	231	1116
39	05514500	Cuivre River near Troy, MO	2339	137	902	207	1131
40	05555500	Vermilion River at Lowell, IL	3310	153	815	174	1046
41	05584500	La Moine River at Colmar, IL	1696	150	897	224	1063
42	05585000	La Moine River at Ripley, IL	3349	131	905	217	1067
43	06191500	Yellowstone River at Corwin Springs MT	6775	1549	700	425	780
44*	06441500	Bad R near Fort Pierre,SD	8151	435	431	17	1083
45*	06847000	Beaver Creek near Beaver City, Nebr.	5387	660	500	7	1240
46	06885500	Black Vermillion R Nr Frankfort, KS	1062	337	814	120	1130
47	06888500	Mill C Nr Paxico, KS	824	293	862	177	1146
48	06892000	Stranger C Nr Tonganoxie, KS	1052	244	954	221	1137
49	06928000	Gasconade River near Hazelgreen, MO	3237	258	983	228	1201
50	07049000	War Eagle Creek near Hindsville, AR	681	356	1083	371	1276
51	07056000	Buffalo River near St. Joe, AR	2147	171	1083	366	1194
52	07057500	North Fork River near Tecumseh, MO	1453	178	997	390	1252
53	07058000	Bryant Creek near Tecumseh, MO	1476	175	997	267	1252
54	07067000	Current River at Van Buren, MO	4318	135	1010	333	1241
55	07068000	Current River at Doniphan, MO	5278	98	1023	398	1256
56	07072000	Eleven Point River near Ravenden Springs, AR	2927	89	1055	308	1281
57	07197000	Baron Fork at Eldon, OK	808	214	1064	258	1250
58*	07222500	Conchas River at Variadero, NM	1355	1351	369	7	1372
59	07252000	Mulberry River near Mulberry, AR	966	132	1180	426	1264
60	07261000	Cadron Creek near Guy, AR	438	113	1182	545	1331
61	08171300	Blanco Rv Nr Kyle, TX	1067	189	816	103	1498
62*	08189500	Mission Rv at Refugio, TX	1787	0	830	63	1547
63*	08340500	Arroyo Chico Nr Guadalupe, NM	3600	1805	247	5	1264
64*	09430500	Gila River near Gila, NM	4828	1419	491	28	1310
65	11080500	Ef San Gabriel R Nr Camp Bonita CA	219	478	784	319	1078
66	11138500	Sisquoc R Nr Sisquoc CA	728	190	403	82	1376
67	11213500	Kings R Ab Nf Nr Trimmer CA	2466	305	800	559	848
68*	11224500	Los Gatos C Ab Nunez Cyn Nr Coalinga CA	248	325	428	21	1332
69	11281000	Sf Tuolumne R Nr Oakland Recreation Camp CA	225	854	978	429	1121
70#	11355500	Hat C Nr Hat Creek CA	420	1311	1227	313	1019
71	11532500	Smith R Nr Crescent City CA	1590	24	2686	2133	1050
72	12358500	M F Flathead River near West Glacier MT	2914	954	1116	928	763
73	12413000	Nf Coeur D Alene River at Enaville ID	2318	640	1108	753	894
74	13337000	Lochsa River Nr Lowell ID	3051	443	1291	896	835
75	13340500	Nf Clearwater River at Bungalow Ranger Station ID	2586	683	1537	957	854
76	14101500	White River Below Tygh Valley, Oreg.	1080	265	760	329	937
77	14232500	Cispus River near Randle, WA	831	372	2010	1432	832

M.A. = mean annual

\* = Watershed removed, runoff ration < 0.1

# = Watershed removed, no parameter set produces NSE >0

Table A: Information of watersheds used in the study.

ID	USGS ID	LAI		Sb		Fc		ASS		ABF	
		Lower	Upper	Lower	Upper	Lower	Upper	Lower	Upper	Lower	Upper
01	1138000	0	12.22704	310	872	0.265	0.722	0.035579	0.156145	0.017771	0.021777
02	1514000	0	6.2458	306	859	0.265	0.722	0.043073	0.186071	0.007022	0.009227
03	1543500	0	7.9792	330	930	0.204	0.56	0.057408	0.196417	0.005843	0.035326
04	1548500	0	6.86652	306	858	0.225	0.611	0.0276	0.131921	0.003745	0.011609
05	1606500	0	6.13036	255	715	0.225	0.611	0.019338	0.122623	0.004286	0.009612
06	1611500	0	6.03572	223	626	0.183	0.5	0.021073	0.110809	0.003005	0.008359
07	1663500	0	5.36328	313	879	0.285	0.78	0.024524	0.105462	0.007127	0.010629
08	1664000	0	4.68336	313	876	0.285	0.78	0.019207	0.080578	0.002839	0.010548
09	1667500	0	4.79184	358	1003	0.285	0.78	0.024211	0.077797	0.011533	0.023306
10	2016000	0	7.83216	221	618	0.204	0.56	0.023361	0.100001	0.006681	0.017158
11	2018000	0	6.37448	247	692	0.224	0.611	0.030845	0.106316	0.008289	0.019007
12	2030500	0	8.75112	356	1000	0.306	0.833	0.021063	0.10079	0.011229	0.017353
13	2143000	0	6.86696	336	942	0.285	0.778	0.048124	0.161928	0.026657	0.064391
14	2472000	0.5	9.88832	375	1050	0.306	0.833	0.027481	0.16287	0.004434	0.013645
15	2479300	0.5	8.57836	381	1067	0.285	0.778	0.02899	0.115484	0.007829	0.019957
16	3069500	0	8.46072	250	701	0.225	0.611	0.079732	0.272717	0.016562	0.038479
17	3070000	0	7.81944	243	680	0.225	0.611	0.064511	0.260856	0.010598	0.031818
18	3114500	9	5.34424	250	702	0.265	0.722	0.022733	0.13807	0.001604	0.005186
19	3155500	0	5.40644	245	695	0.265	0.722	0.026432	0.140267	0.001582	0.004446
20	3161000	0	5.23724	356	998	0.265	0.722	0.043081	0.105708	0.018673	0.047598
21	3164000	0	4.85712	352	988	0.265	0.723	0.037687	0.114855	0.014055	0.027477
22	3173000	0	5.5628	279	781	0.225	0.611	0.024066	0.094826	0.006672	0.011218
23	3180500	0	7.2706	236	663	0.204	0.556	0.040757	0.190844	0.003852	0.019285
24	3182500	0	6.95412	235	656	0.204	0.556	0.044959	0.188474	0.007334	0.011495
25	3186500	0	8.77724	258	725	0.245	0.667	0.074897	0.244868	0.01019	0.016059
26	3213000	0	5.53516	276	774	0.204	0.556	0.039699	0.110225	0.01227	0.029752
27	3237500	0	3.5816	304	854	0.285	0.778	0.0165	0.112836	0.003358	0.005948
28	3238500	0	1.50316	376	1055	0.367	1	0.029633	0.121546	0.00266	0.008589
29	3281500	0	5.2422	245	685	0.265	0.722	0.032509	0.152908	0.00295	0.010232
30	3346000	0	1.029	381	1067	0.367	1	0.015521	0.073177	0.00282	0.013033
31	3473000	0	5.10284	290	814	0.245	0.667	0.036357	0.134467	0.010941	0.023753
32	3490000	0	4.67592	280	783	0.245	0.667	0.035748	0.14784	0.004969	0.013829
33	3504000	0	5.911	346	970	0.265	0.723	0.080578	0.162394	0.030514	0.047114
34	3574500	0	5.7902	243	680	0.245	0.667	0.050638	0.252672	0.007678	0.014482
35	5408000	0	2.7668	278	780	0.326	0.89	0.023649	0.115273	0.01151	0.03083
36	5412500	0	0.69396	357	1000	0.367	1	0.01544	0.054232	0.003218	0.006131
37	5502040	0	1.95936	381	1067	0.408	1.11	0.030736	0.122481	0.006255	0.016266
38	5507500	0	0.91844	380	1064	0.306	0.833	0.013702	0.087733	0.000928	0.00308
39	5514500	0	1.42624	361	1011	0.306	0.833	0.013434	0.066811	0.001135	0.004746
40	5555500	0	0.1146	381	1067	0.346	0.945	0.016763	0.057306	0.003041	0.011177
41	5584500	0	0.99816	318	1067	0.387	1.06	0.016505	0.081104	0.001051	0.004159
42	5585000	0	1.33416	381	1067	0.387	1.06	0.015875	0.073742	0.002409	0.003535
43	6191500	0.5	8.88468	305	855	0.143	0.389	0.019338	0.075167	0.005507	0.015386
44	6441500	0	0.00756	230	645	0.347	0.945	0.002621	0.013884	0.000256	0.000578
45	6847000	0	0.003	378	1060	0.408	1.11	0.000938	0.004333	0.00026	0.001386
46	6885500	0	0.41608	375	1052	0.306	0.833	0.008543	0.041513	0.00119	0.002453
47	6888500	0	1.12756	261	732	0.265	0.722	0.010617	0.049041	0.005216	0.008292
48	6892000	0	1.0274	360	1008	0.346	0.944	0.014462	0.076442	0.001512	0.005457
49	6928000	0	3.44332	360	1009	0.183	0.5	0.019858	0.071708	0.002131	0.003507
50	7049000	0	3.8712	293	820	0.204	0.556	0.027829	0.117023	0.003725	0.007225
51	7056000	0	5.88428	291	815	0.225	0.611	0.034855	0.13253	0.002795	0.005929
52	7057500	0	4.9406	334	938	0.204	0.556	0.016052	0.061916	0.005126	0.014191
53	7058000	0	4.62456	364	1021	0.204	0.556	0.01502	0.057126	0.003705	0.005447
54	7067000	0	6.32288	357	1000	0.204	0.556	0.023457	0.066938	0.00245	0.006782
55	7068000	0	6.4624	357	1002	0.204	0.556	0.01609	0.071212	0.008394	0.037073
56	7072000	0	4.86192	310	872	0.245	0.667	0.010757	0.042557	0.005419	0.008481
57	7197000	0	3.33572	310	953	0.225	0.611	0.020989	0.07265	0.004233	0.009389
58	7222500	0	1.87296	255	714	0.306	0.833	0.003203	0.007704	0.000284	0.00093
59	7252000	0	7.5112	266	747	0.225	0.611	0.038927	0.184329	0.002294	0.006594
60	7261000	0	6.30308	205	574	0.225	0.611	0.033282	0.181029	0.003295	0.004527
61	8171300	0.5	7.72348	224	629	0.245	0.667	0.006152	0.02304	0.001442	0.003983
62	8189500	0	0.58296	310	872	0.265	0.722	0.008912	0.036877	0.001364	0.003862
63	8340500	0	2.95272	291	817	0.285	0.778	0.002059	0.012444	0.000147	0.001018
64	9430500	0	4.3506	267	750	0.225	0.611	0.001991	0.006002	0.000791	0.002405
65	11080500	0.5	8.07024	152	426	0.143	0.389	0.011163	0.081193	0.003991	0.027592
66	11138500	0	5.12776	132	372	0.306	0.833	0.001917	0.028929	0.00027	0.002382
67	11213500	0.5	8.86104	308	865	0.143	0.389	0.020656	0.150054	0.004909	0.018084
68	11224500	0	1.9664	212	595	0.285	0.778	0.00577	0.020251	0.001551	0.003217
69	11281000	0.5	19.11028	327	918	0.225	0.611	0.036522	0.135997	0.003386	0.015681
70	11355500	0.5	16.60176	312	875	0.225	0.611	0.025034	0.052713	0.01551	0.023702
71	11532500	0.5	16.83636	249	700	0.225	0.611	0.104577	0.708138	0.006403	0.017167
72	12358500	0.5	16.05776	310	872	0.184	0.5	0.041778	0.171636	0.011268	0.023894
73	12413000	0.5	20.21824	372	1042	0.184	0.5	0.049911	0.180239	0.007186	0.013014
74	13337000	0.5	18.82644	250	701	0.204	0.556	0.045206	0.211898	0.008259	0.026454
75	13340500	0.5	16.81392	325	911	0.204	0.556	0.066364	0.200987	0.018093	0.034445
76	14101500	0.5	11.31032	270	760	0.265	0.722	0.019507	0.0607	0.008024	0.020055
77	14232500	0.5	17.13952	344	965	0.225	0.611	0.086241	0.268891	0.035902	0.061366

Table B: Ranges of parameters obtained from *a priori* parameter estimation for all watersheds.

# References

- [1] C. J. Vörösmarty, P. Green, J. Salisbury, and R. B. Lammers. Global water resources: vulnerability from climate change and population growth. *science* 289, (2000) 284–288.
- [2] D. Legesse, C. Vallet-Coulomb, and F. Gasse. Hydrological response of a catchment to climate and land use changes in Tropical Africa: case study South Central Ethiopia. *Journal of Hydrology* 275, (2003) 67–85.
- [3] N. W. Arnell. Climate change and global water resources: SRES emissions and socio-economic scenarios. *Global environmental change* 14, (2004) 31–52.
- [4] G. Sun, S. G. McNulty, J. M. Myers, and E. C. Cohen. Impacts of climate change, population growth, land use change, and groundwater availability on water supply and demand across the conterminous US. *AWRA Hydrology & Watershed Management Technical Committee* .
- [5] A. A. Anandhi, N. N. Omani, I. Chaubey, R. Horton, D. Bader, and R. Nanjundiah. What changes do the CMIP5 climate models predict for South Asia and what are some potential impacts on managed ecosystems and water resources. In *ASABE 1st Climate Change Symposium: Adaptation and Mitigation Conference Proceedings*. American Society of Agricultural and Biological Engineers, 2015 1–4.
- [6] G. Watts, R. W. Battarbee, J. P. Bloomfield, J. Crossman, A. Daccache, I. Durance, J. A. Elliott, G. Garner, J. Hannaford, D. M. Hannah et al. Climate change and water in the UK—past changes and future prospects. *Progress in Physical Geography* 39, (2015) 6–28.
- [7] J. Henderson, C. Rodgers, R. Jones, J. Smith, K. Strzepek, and J. Martinich. Economic impacts of climate change on water resources in the coterminous

- United States. *Mitigation and Adaptation Strategies for Global Change* 20, (2015) 135–157.
- [8] C. Chen, S. Hagemann, and J. Liu. Assessment of impact of climate change on the blue and green water resources in large river basins in China. *Environmental Earth Sciences* 74, (2015) 6381–6394.
- [9] A. W. Wood, L. R. Leung, V. Sridhar, and D. Lettenmaier. Hydrologic implications of dynamical and statistical approaches to downscaling climate model outputs. *Climatic change* 62, (2004) 189–216.
- [10] C. Tebaldi, R. L. Smith, D. Nychka, and L. O. Mearns. Quantifying uncertainty in projections of regional climate change: A Bayesian approach to the analysis of multimodel ensembles. *Journal of Climate* 18, (2005) 1524–1540.
- [11] H. G. Hidalgo, M. D. Dettinger, and D. R. Cayan. Downscaling with constructed analogues: Daily precipitation and temperature fields over the United States. *California Energy Commission PIER Final Project Report CEC-500-2007-123* .
- [12] C. Dobler, S. Hagemann, R. Wilby, and J. Stötter. Quantifying different sources of uncertainty in hydrological projections in an Alpine watershed. *Hydrology and Earth System Sciences* 16, (2012) 4343–4360.
- [13] T. Bosshard, M. Carambia, K. Goergen, S. Kotlarski, P. Krahe, M. Zappa, and C. Schär. Quantifying uncertainty sources in an ensemble of hydrological climate-impact projections. *Water Resources Research* 49, (2013) 1523–1536.
- [14] N. Addor, T. Ewen, L. Johnson, A. Çöltekin, C. Derungs, and V. Muccione. From products to processes: Academic events to foster interdisciplinary and iterative dialogue in a changing climate. *Earth's Future* 3, (2015) 289–297.
- [15] I. Giuntoli, J. Vidal, C. Prudhomme, and D. Hannah. Future hydrological extremes: the uncertainty from multiple global climate and global hydrological models. *Earth System Dynamics* 6, (2015) 267.
- [16] T. Vetter, S. Huang, V. Aich, T. Yang, X. Wang, V. Krysanova, and F. Hattermann. Multi-model climate impact assessment and intercomparison for three large-scale river basins on three continents. *Earth System Dynamics* 6, (2015) 17.

- [17] J. Schewe, J. Heinke, D. Gerten, I. Haddeland, N. W. Arnell, D. B. Clark, R. Dankers, S. Eisner, B. M. Fekete, F. J. Colón-González et al. Multimodel assessment of water scarcity under climate change. *Proceedings of the National Academy of Sciences* 111, (2014) 3245–3250.
- [18] R. Singh, T. Wagener, R. Crane, M. Mann, and L. Ning. A vulnerability driven approach to identify adverse climate and land use change combinations for critical hydrologic indicator thresholds: Application to a watershed in Pennsylvania, USA. *Water Resources Research* 50, (2014) 3409–3427.
- [19] A. Sankarasubramanian, R. M. Vogel, and J. F. Limbrunner. Climate elasticity of streamflow in the United States. *Water Resources Research* 37, (2001) 1771–1781.
- [20] M. Staudinger, M. Weiler, and J. Seibert. Quantifying sensitivity to droughts: an experimental modeling approach. *Hydrology and Earth System Sciences* 19, (2015) 1371–1384.
- [21] C. Mateus, D. D. Tullios, and C. G. Surfleet. Hydrologic Sensitivity to Climate and Land Use Changes in the Santiam River Basin, Oregon. *JAWRA Journal of the American Water Resources Association* 51, (2015) 400–420.
- [22] W. R. Berghuijs, A. Hartmann, and R. A. Woods. Streamflow sensitivity to water storage changes across Europe. *Geophysical Research Letters* 43, (2016) 1980–1987.
- [23] C. Rougé, J.-D. Mathias, and G. Deffuant. Vulnerability: From the conceptual to the operational using a dynamical system perspective. *Environmental Modelling & Software* 73, (2015) 218–230.
- [24] S. Banks. Exploratory modeling for policy analysis. *Operations research* 41, (1993) 435–449.
- [25] R. J. Lempert, B. P. Bryant, and S. C. Banks. Comparing algorithms for scenario discovery. *RAND, Santa Monica* .
- [26] C. Brown, W. Werick, W. Leger, and D. Fay. A Decision-Analytic approach to managing climate risks: Application to the upper great Lakes<sup>1</sup>. *JAWRA Journal of the American Water Resources Association* 47, (2011) 524–534.

- [27] C. Brown, Y. Ghile, M. Laverty, and K. Li. Decision scaling: Linking bottom-up vulnerability analysis with climate projections in the water sector. *Water Resources Research* 48.
- [28] F. Boso, F. Barros, A. Fiori, and A. Bellin. Performance analysis of statistical spatial measures for contaminant plume characterization toward risk-based decision making. *Water Resources Research* 49, (2013) 3119–3132.
- [29] A. Khader, D. E. Rosenberg, and M. McKee. A decision tree model to estimate the value of information provided by a groundwater quality monitoring network. *Hydrology and Earth System Sciences* 17, (2013) 1797–1807.
- [30] H. Kunreuther, G. Heal, M. Allen, O. Edenhofer, C. B. Field, and G. Yohe. Risk management and climate change. *Nature Climate Change* 3, (2013) 447–450.
- [31] P. Moody and C. Brown. Robustness indicators for evaluation under climate change: Application to the upper Great Lakes. *Water Resources Research* 49, (2013) 3576–3588.
- [32] C. P. Weaver, R. J. Lempert, C. Brown, J. A. Hall, D. Revell, and D. Sarewitz. Improving the contribution of climate model information to decision making: the value and demands of robust decision frameworks. *Wiley Interdisciplinary Reviews: Climate Change* 4, (2013) 39–60.
- [33] N. L. Poff, C. M. Brown, T. E. Grantham, J. H. Matthews, M. A. Palmer, C. M. Spence, R. L. Wilby, M. Haasnoot, G. F. Mendoza, K. C. Dominique et al. Sustainable water management under future uncertainty with eco-engineering decision scaling. *Nature Climate Change* .
- [34] D. Farmer, M. Sivapalan, and C. Jothityangkoon. Climate, soil, and vegetation controls upon the variability of water balance in temperate and semiarid landscapes: Downward approach to water balance analysis. *Water Resources Research* 39.
- [35] Y. Bai, T. Wagener, and P. Reed. A top-down framework for watershed model evaluation and selection under uncertainty. *Environmental Modelling & Software* 24, (2009) 901–916.
- [36] F. L. Zhao, Zhang and Zhang. The Xinanjiang model, in Proceedings of the Symposium on the Application of Recent Developments in Hydrological. .

- [37] K. A. Sawicz. Catchment classification-understanding hydrologic similarity through catchment function. THE PENNSYLVANIA STATE UNIVERSITY, 2013.
- [38] J. D. Olden and N. Poff. Redundancy and the choice of hydrologic indices for characterizing streamflow regimes. *River Research and Applications* 19, (2003) 101–121.
- [39] I. Nalbantis and G. Tsakiris. Assessment of hydrological drought revisited. *Water Resources Management* 23, (2009) 881–897.
- [40] K. G. Ries. August median streamflows in Massachusetts. US Department of the Interior, US Geological Survey, 1997.
- [41] N. L. Poff, B. D. Richter, A. H. Arthington, S. E. Bunn, R. J. Naiman, E. Kendy, M. Acreman, C. Apse, B. P. Bledsoe, M. C. Freeman et al. The ecological limits of hydrologic alteration (ELOHA): a new framework for developing regional environmental flow standards. *Freshwater Biology* 55, (2010) 147–170.
- [42] L. Breiman, J. Friedman, C. J. Stone, and R. A. Olshen. Classification and regression trees. CRC press, 1984.
- [43] T. M. Therneau, B. Atkinson, and B. Ripley. rpart: Recursive Partitioning. R package version 3.1-46. *Computer software program retrieved from <http://CRAN.R-project.org/package=rpart>* .
- [44] Q. Duan, J. Schaake, V. Andreassian, S. Franks, G. Goteti, H. Gupta, Y. Gusev, F. Habets, A. Hall, L. Hay et al. Model Parameter Estimation Experiment (MOPEX): An overview of science strategy and major results from the second and third workshops. *Journal of Hydrology* 320, (2006) 3–17.
- [45] R. Singh, S. Archfield, and T. Wagener. Identifying dominant controls on hydrologic parameter transfer from gauged to ungauged catchments—A comparative hydrology approach. *Journal of Hydrology* 517, (2014) 985–996.
- [46] J. A. Falcone, D. M. Carlisle, D. M. Wolock, and M. R. Meador. GAGES: A stream gage database for evaluating natural and altered flow conditions in the conterminous United States: Ecological Archives E091-045. *Ecology* 91, (2010) 621–621.

- [47] G. Van Oldenborgh, M. Collins, J. Arblaster, J. Christensen, J. Marotzke, S. Power, M. Rummukainen, and T. Zhou. Annex I: atlas of global and regional climate projections. *Climate change* 1311–1393.
- [48] K. van Werkhoven, T. Wagener, P. Reed, and Y. Tang. Characterization of watershed model behavior across a hydroclimatic gradient. *Water Resources Research* 44.
- [49] J. Kollat, P. Reed, and T. Wagener. When are multiobjective calibration trade-offs in hydrologic models meaningful? *Water Resources Research* 48.
- [50] C. Kelleher, T. Wagener, B. McGlynn, A. Ward, M. Gooseff, and R. Payn. Identifiability of transient storage model parameters along a mountain stream. *Water Resources Research* 49, (2013) 5290–5306.
- [51] M. Krzywinski, J. Schein, I. Birol, J. Connors, R. Gascoyne, D. Horsman, S. J. Jones, and M. A. Marra. Circos: an information aesthetic for comparative genomics. *Genome research* 19, (2009) 1639–1645.
- [52] M. H. Costa, A. Botta, and J. A. Cardille. Effects of large-scale changes in land cover on the discharge of the Tocantins River, Southeastern Amazonia. *Journal of Hydrology* 283, (2003) 206–217.
- [53] M. Huang, S. Kang, and Y. Li. A comparison of hydrological behaviors of forest and grassland watersheds in gully region of the Loess Plateau. *Journal of Natural Resources* 14, (1999) 226–231.
- [54] Z. Li, W.-z. Liu, X.-c. Zhang, and F.-l. Zheng. Impacts of land use change and climate variability on hydrology in an agricultural catchment on the Loess Plateau of China. *Journal of hydrology* 377, (2009) 35–42.
- [55] S. Dullinger, T. Dirnböck, and G. Grabherr. Modelling climate change-driven treeline shifts: relative effects of temperature increase, dispersal and invasibility. *Journal of ecology* 92, (2004) 241–252.